PROPERTIES OF THE FREQUENCY SVD-DFT METHOD FOR DISCRETE LTV SYSTEMS BASED ON FIRST ORDER EXAMPLES

ORŁOWSKI PRZEMYSŁAW
Technical University of Szczecin, Institute of Control Engineering,
Sikorskiego 37, 70-313 Szczecin, e-mail: orzel@ps.pl

Abstract. The paper develops frequency analysis tools for linear time-varying (LTV), discrete-time systems. The main method is based on the properties of the Singular Value De-composition (SVD), Discrete Fourier Transform (DFT) and Power Spectral Density (PSD). The analysis is carried out for a system with first order dynamics. The general objective of this paper is to examine how system frequency diagrams are depend on the variability of particular parameters. Especially, it is examined how the variability of three matrices of the state space model (scalars, in the 1st order case) influence the approximated Bode diagrams. A few cases of the variability of each matrix, in particular with different frequencies and phase shifting, are considered. Moreover, the analysis is carried out for different cases of the system parameters. The results of analysis for each case are shown in four diagrams: amplitude, phase, impulse and step responses. On the basis of these examples the most important features in each example are characterized.

Key words: Discrete-time systems, Time-varying systems, Non-stationary systems, Frequency methods.

1 INTRODUCTION

The concepts, which are used in the frequency analysis of LTV systems in this work, are based on the idea of connecting the Singular Value Decomposition (SVD), Discrete Fourier Transform (DFT) and the properties of Power Spectral Density (PSD). Until now only a few papers in this field are published see e.g. [Orlowski, 2003, 2004].

The proposed concepts enable to obtain numerically, some equivalents of Bode diagrams for LTV systems. The diagrams have similar properties to classical Bode diagrams for LTI systems. The approximated Bode diagrams are given by a finite set of frequencies (or singular vectors) and their corresponding gains. Of course some information is neglected and some is transcribed into the diagrams. It should be also clear that the information included in diagrams cannot be extracted for specific time samples.

An important advantage of SVD-DFT method is that the results obtained for LTI systems are almost identical as the classical Bode diagrams.

2 MODEL DESCRIPTION

Dynamic, discrete-time system can be given by set of difference equations, called the state space model

$$\mathbf{x}_p(k+1) = \mathbf{A}(k)\cdot\mathbf{x}_p(k) + \mathbf{B}(k)\cdot\mathbf{v}_p(k), \tag{1}$$

$$\mathbf{y}_p(k) = \mathbf{C}(k)\cdot\mathbf{x}_p(k), \quad k\in\mathbf{N}, \quad \mathbf{x}_p(0)=\mathbf{0}, \tag{2}$$

where $\mathbf{x}_p(\cdot)\in(\mathbf{R}^n)^N$ is nominal state, $\mathbf{v}_p(\cdot)\in(\mathbf{R}^m)^N$ is nominal control, $\mathbf{y}_p(\cdot)\in(\mathbf{R}^p)^N$ is nominal output, and $\mathbf{A}(k)\in\mathcal{L}(\mathbf{R}^n)$, $\mathbf{B}(k)\in\mathcal{L}(\mathbf{R}^m,\mathbf{R}^n)$, $\mathbf{C}(k)\in\mathcal{L}(\mathbf{R}^n,\mathbf{R}^p)$ are system's matrices.

Equivalently the system can be given using following operators

$$\hat{\mathbf{y}}_p = \hat{\mathbf{C}}\hat{\mathbf{L}}\hat{\mathbf{B}} \cdot \hat{\mathbf{v}}_p + \hat{\mathbf{C}}\hat{\mathbf{N}} \cdot \mathbf{x}_0 \tag{3}$$

Detailed description of such operators can be found in [Orlowski. 2001, 2004]

3 BODE DIAGRAMS APPROXIMATION

Approximated Bode diagrams follow from the relation between input and output power spectral density and amplitude diagrams. Detailed proof can be found in [Orlowski, 2004]. Amplitude diagram can be approximated by

$$\left|\mathbf{G}(\omega_k)\right| = \sqrt{\frac{1}{N} \cdot \sum_{j=1}^{N} \sigma_j^2 \cdot \left|\mathrm{DFT_k}[\mathbf{u}_j]\right|^2} \tag{4}$$

and similarly the phase diagram by

$$\varphi(\omega_k) = \arg\left(\sum_{j=1}^{N} \sigma_j \cdot \frac{\mathrm{DFT_k}[\mathbf{u}_j]}{\mathrm{DFT_k}[\mathbf{v}_j]} \right) \tag{5}$$

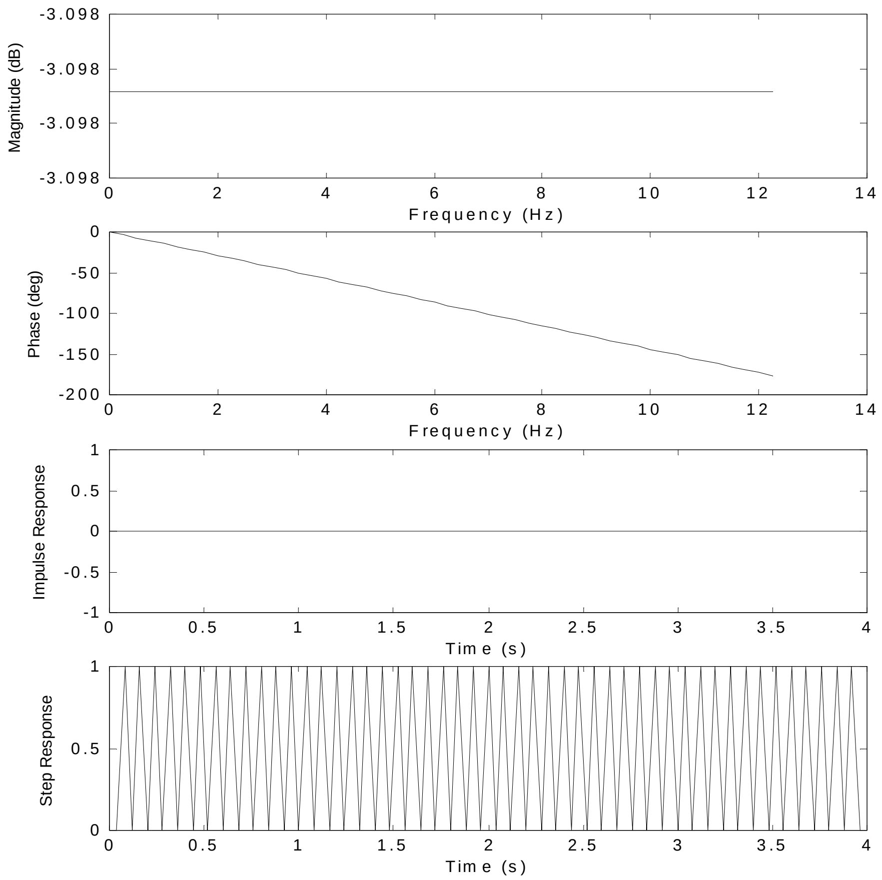

Figure 1. Bode diagrams, impulse and step responses for delay system.

4 SELECTED PROPERTIES OF 1ST ORDER LTV SYSTEM

Selected results of frequency diagrams approximation for discrete-time LTV system with first order dynamics using discrete operators, SVD-DFT are presented below. In all examples sampling period T_p=0.04 and simulation horizon N=100. As the variability function for time-varying (TV) system matrices have been chosen rectangular function (RF) $\Pi\left(\frac{k}{T}\right)$ having two levels: lower equal to zero and higher equal to 1. The wave starts from lower level with period T and filling 50%.

For all examples there are computed and plotted four diagrams: amplitude, phase, impulse and step responses.

4.1 Delay system with TV input matrix

First simulation has been carried out for simple one sample delay system given by following one dimension matrices of the model (1-2).

$$\mathrm{A}(k) = 0,\ \mathrm{B}(k) = \Pi\left(\frac{k}{2}\right),\ \mathrm{C}(k) = 1 \tag{6}$$

Corresponding diagrams are plotted on fig. 1. Amplification level on amplitude diagram is equal to –3dB. Such value is a result of lower power of signal B(k) then for ones signal. The B(k) signal has $\sqrt{2}$ times less energy than ones signal, what corresponds in –3 dB damping of magnitude.

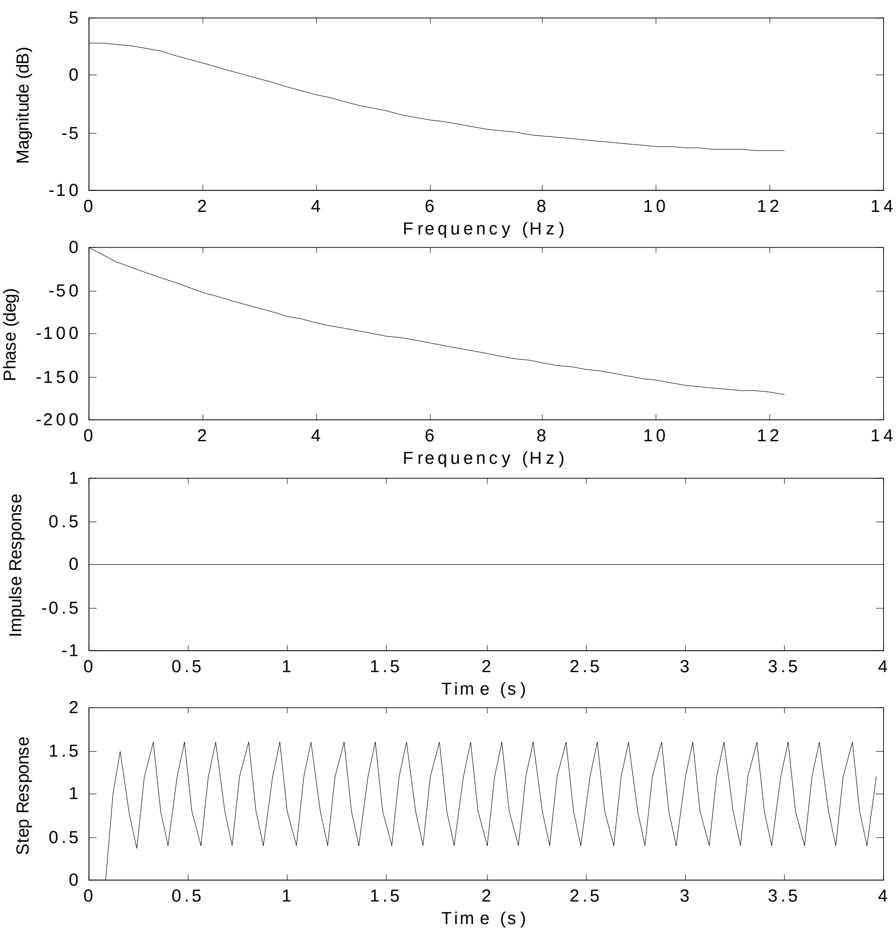

Figure 2. Bode diagrams, impulse and step responses for inertial system with TV input matrix.

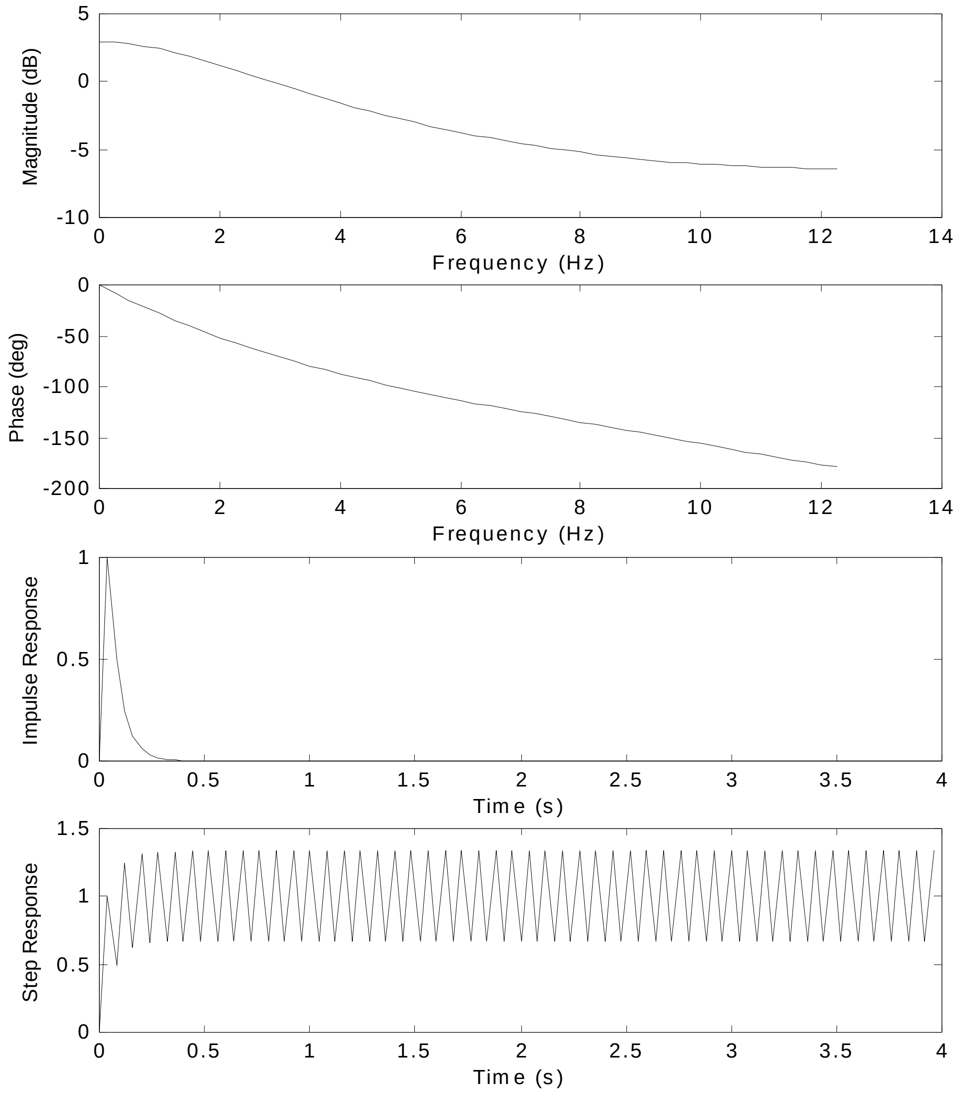

Figure 3. Bode diagrams, impulse and step responses for system with TV shifted input matrix and A(*k*)=0.5.

4.2 Inertial system with TV input matrix

Following simulation has been carried with changed values of matrix A and period of B.

$$\mathrm{A}(k) = 0.5,\ \mathrm{B}(k) = \Pi\left(\frac{k}{4}\right),\ \mathrm{C}(k) = 1 \tag{7}$$

Corresponding diagrams shows fig. 2. In general they are similar to LTI case with B=1. The difference is similar to example 1: an amplitude diagram is damped by 3 dB (expected starting level for LTI system is equal to 6 dB). Such damping is caused by the power's change of B(*k*) signal. Other important fact is that the period *T* of B(*k*) does not influence on the diagrams.

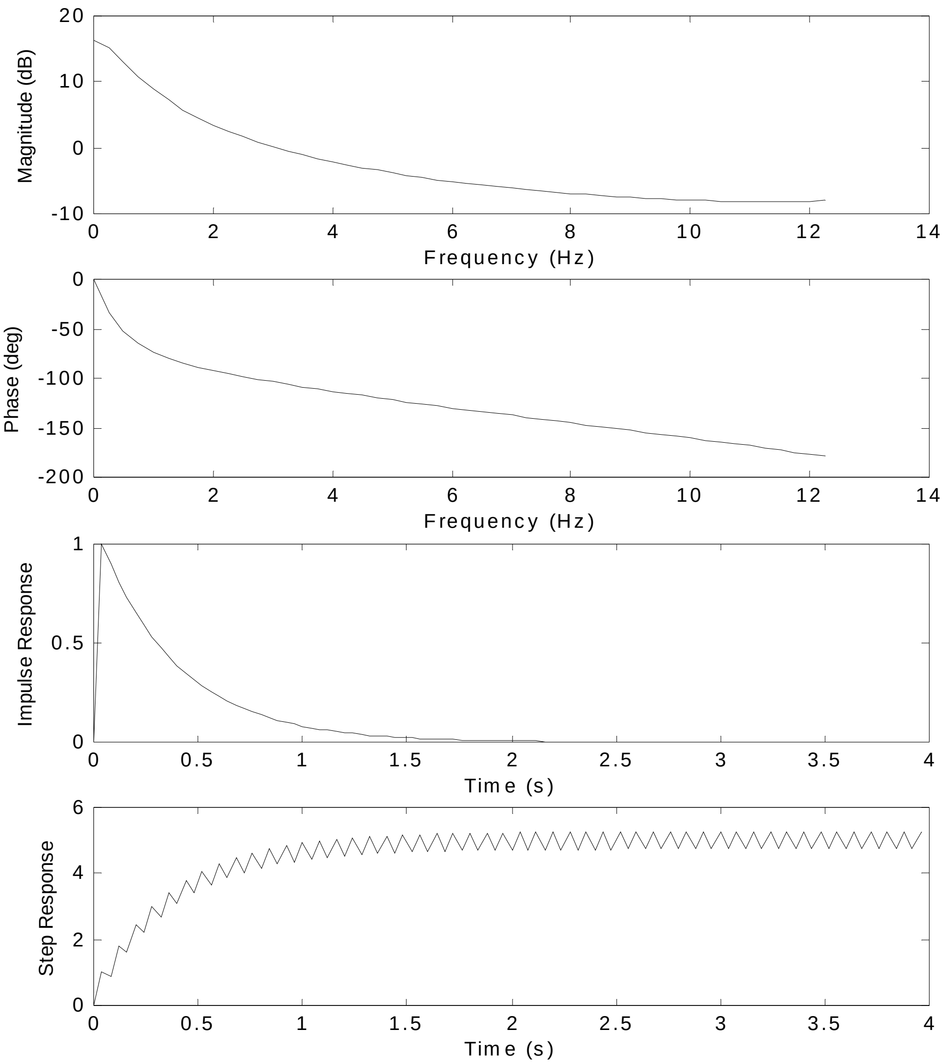

Figure 4. Bode diagrams, impulse and step responses for system with TV shifted input matrix and A(k)=0.9.

4.3 System with TV shifted input matrix

Now the example from section 4.2 is modified by change in period and time shift in $\mathbf{B}(k)$ matrix. System matrices are following.

$$\mathrm{A}(k)=0.5,\ \mathrm{B}(k)=\Pi\left(\frac{k+1}{2}\right),\ \mathrm{C}(k)=1 \tag{8}$$

Corresponding diagrams shows fig. 3. Comparing this example to previous one it can be seen that not only amplitude but also phase of $\mathbf{B}(k)$ matrix does not influence Bode SVD-DFT diagrams. Changes are visible only on step responses.

In the case when only B matrix is time varying, Bode diagrams are very similar to LTI case. For better evaluation there are analysed two similar examples. First with A(k)=0.9 and second with A(k)=-0.5. Figs. 4 and 5 shows diagrams and responses for the first and second system respectively.

If the system has negative amplification in steady state, there will be change on phase plot similar to LTI case, e.g. 180 degrees shift for frequency f=0.

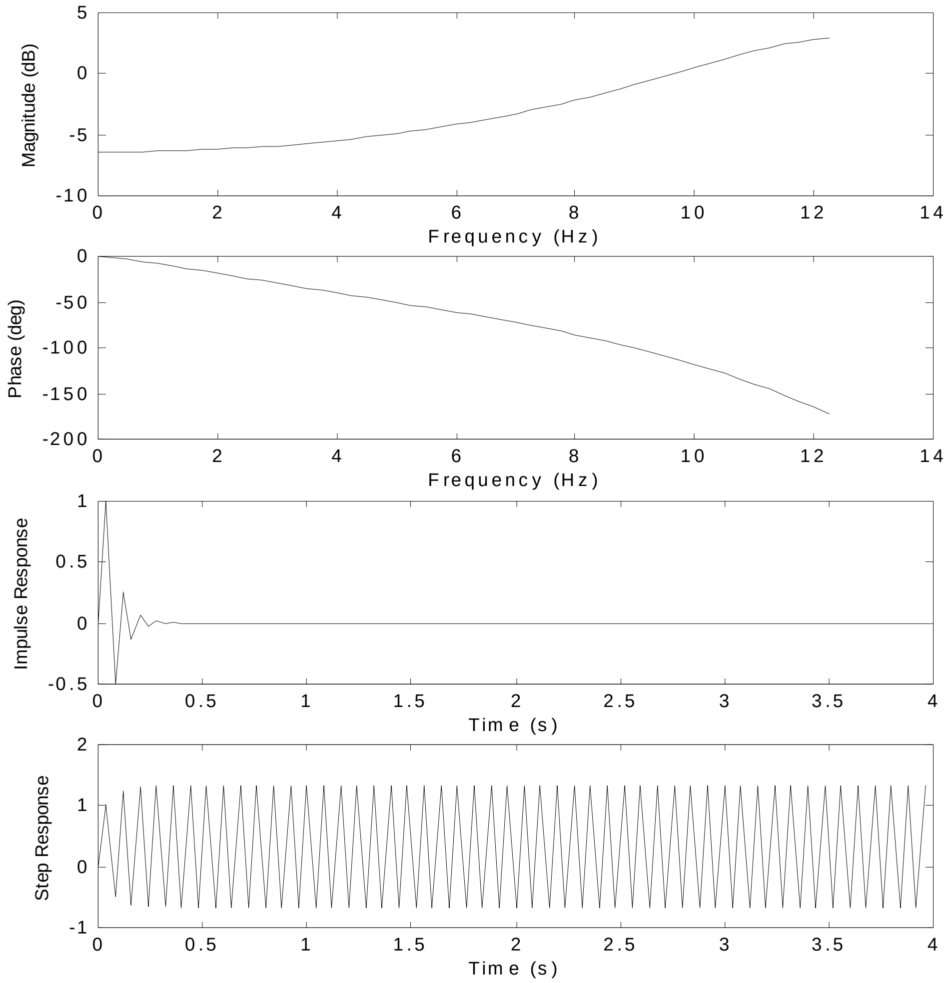

Figure 5. Bode diagrams, impulse and step responses for system with TV input matrix and A(k)=-0.5.

Generalization of such system in LTV case can be negative system, which must have negative amplification for f=0 or in case of average steady state amplification equal to zero at least negative initial tendency.

4.4 System with TV balanced input matrix

Special case of modulation with time and amplitude shifting is input balanced modulation, which can be obtained by modification of **B**(k) matrix.

$$\mathrm{A}(k) = 0.5,\ \mathrm{B}(k) = \Pi\left(\frac{k}{2}\right) - 0.5,\ \mathrm{C}(k) = 1 \tag{9}$$

Corresponding diagrams are plotted on fig. 6. Signal **B**(k) is symmetrical thus the modulation is balanced. Moreover **B**(k) begins from –0.5, thus system is negative.

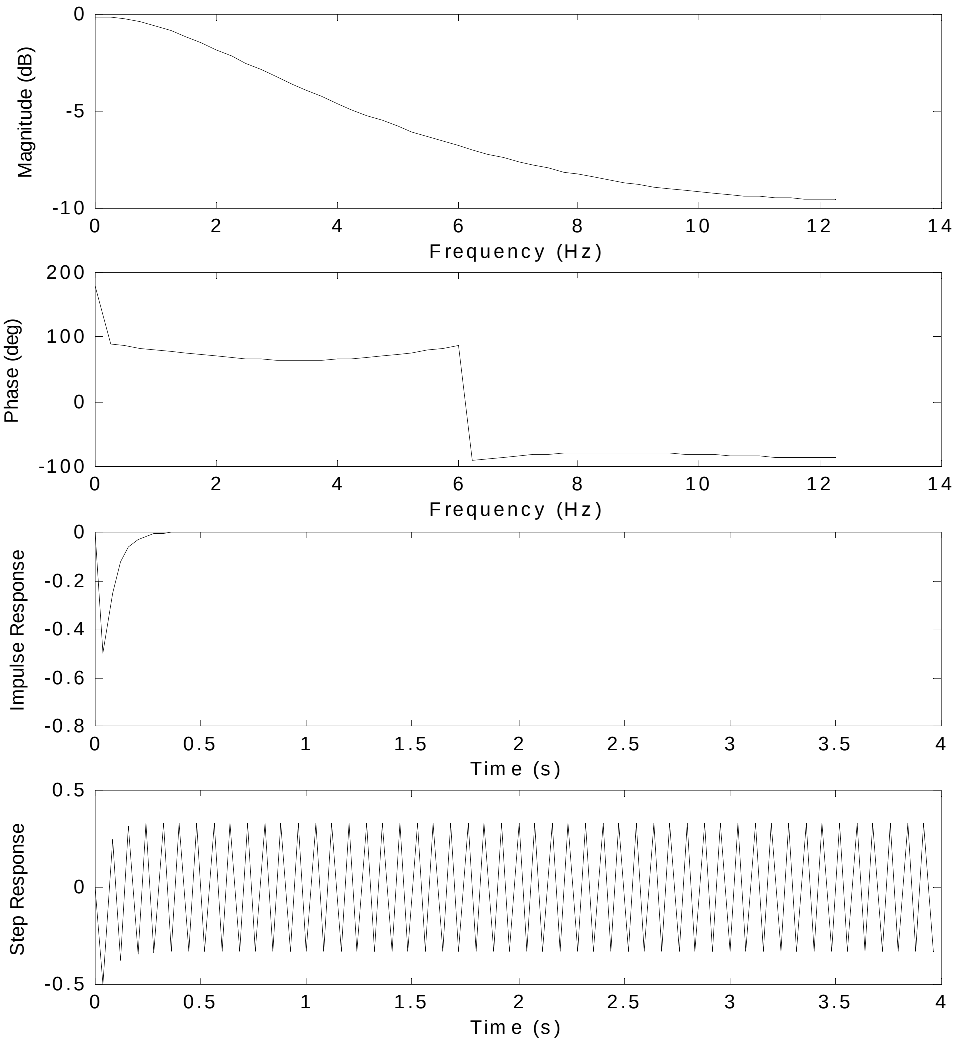

Figure 6. Bode diagrams, impulse and step responses for system with TV balanced input matrix, period of B(k) 2 samples (T=0.08 s) and A(k)=0.5.

Analysis of the responses from fig. 6 follows to following conclusions:

a) Symmetry in **B**(k) results in nearly symmetrical phase plot

b) Negative tendency in impulse and step responses results in 180 deg shift for f nearly zero

c) Lower power of signal **B**(k) (2 times less then for examples 4.2-3) results in additive 3 dB damping (jointly –6 dB).

It should be also noted that for balanced modulation the beginning of phase diagrams is dependent on time shift of the **B**(k) signal.

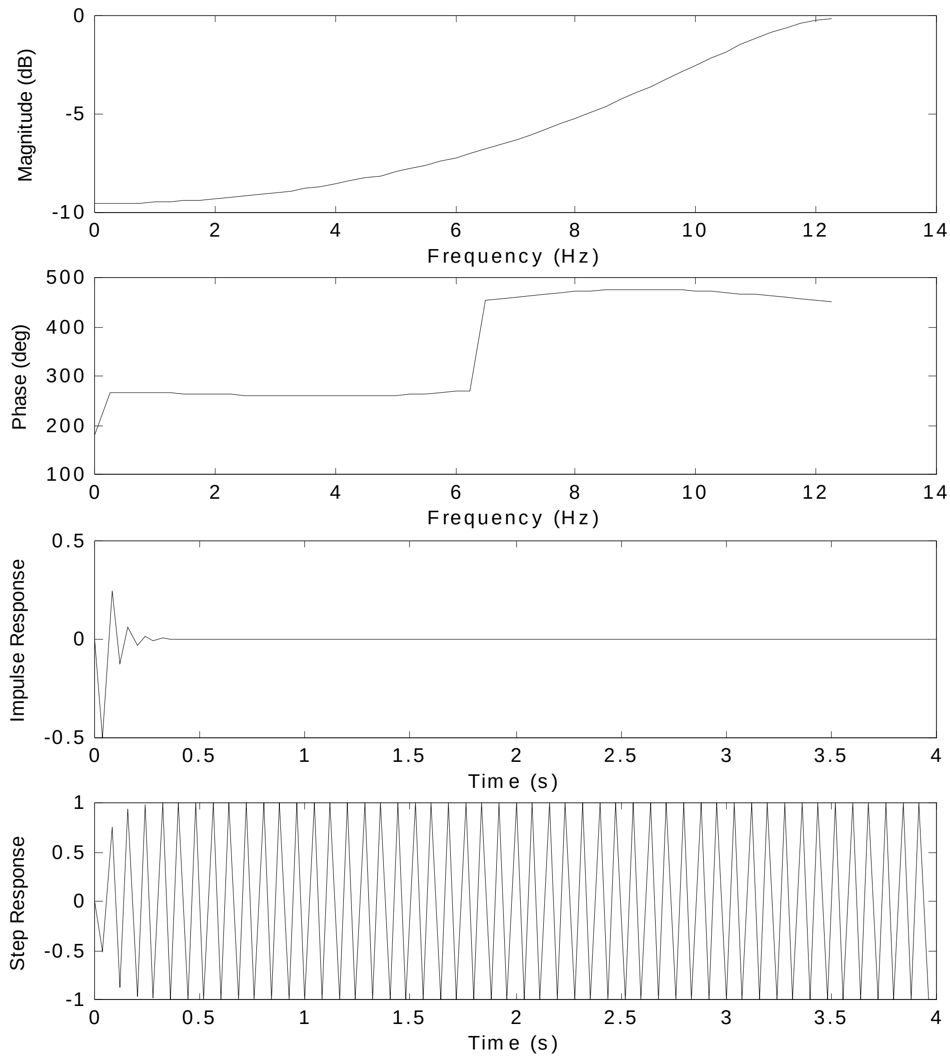

Figure 7. Bode diagrams, impulse and step responses for system with TV balanced input matrix period 2 samples (T=0.08 s) and A(k)=-0.5.

Similar analysis can be carried out for the same case with only changed matrix A(k)=-0.5. Fig. 7 shows diagrams and responses for such system. Bode diagrams are different then for previous case, but phase plot still has symmetry (axis of symmetry 360 deg).

After two-times increased period of **B**(k) signal, system matrices take the following form.

$$\mathrm{A}(k) = 0.5,\ \mathrm{B}(k) = \Pi\left(\frac{k}{4}\right) - 0.5,\ \mathrm{C}(k) = 1 \tag{10}$$

Corresponding diagrams are plotted on fig. 8. Some similarities can be seen on fig. 6, especially amplitude diagrams are identical and the phase plot are almost symmetrical. The only significant difference is 2 times increased number of transitions on phase diagram. The number is of course proportional to the period of **B**(k) signal.

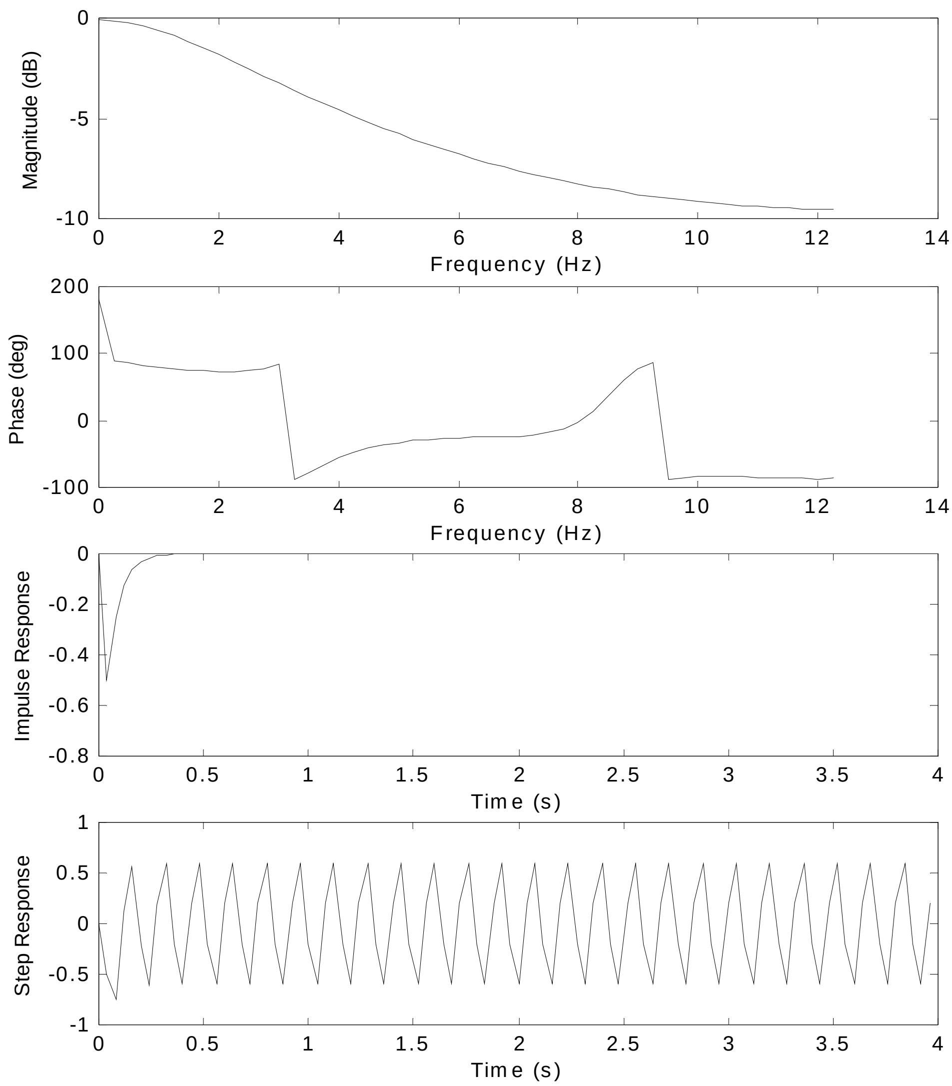

Figure 8. Bode diagrams, impulse and step responses for system with TV balanced input matrix period of B(*k*) 4 samples (*T*=0.16 s) and A(*k*)=0.5.

Examples 4.1-4 are concerned on a case when matrix **B**(*k*) is time dependent only. In such case input signal is modulated and thus is filtered by the dynamics of the system. Although different situation take place when matrices **C**(*k*) and/or **A**(*k*) are time dependent. Time dependent matrix **C**(*k*) is a particular case when input signal is filtered by system dynamics and then modulated by **C**(*k*), while varying matrix **B**(*k*) modulate input signal before filtering. Some important differences follows both in properties of the system and form of the diagrams.

4.5 System with TV output matrix

Following model is borrowed from example 4.2 with only changes in matrices **B** and **C**.

$$\mathrm{A}(k) = 0.5,\ \mathrm{B}(k) = 1,\ \mathrm{C}(k) = \Pi\left(\frac{k}{4}\right) \tag{11}$$

Corresponding diagrams for horizon N=200 steps are depicted on fig. 9. Comparison to fig. 2 shows that not only amplitude diagram is drastically changed but also significant changes are visible on impulse and step responses of the system.

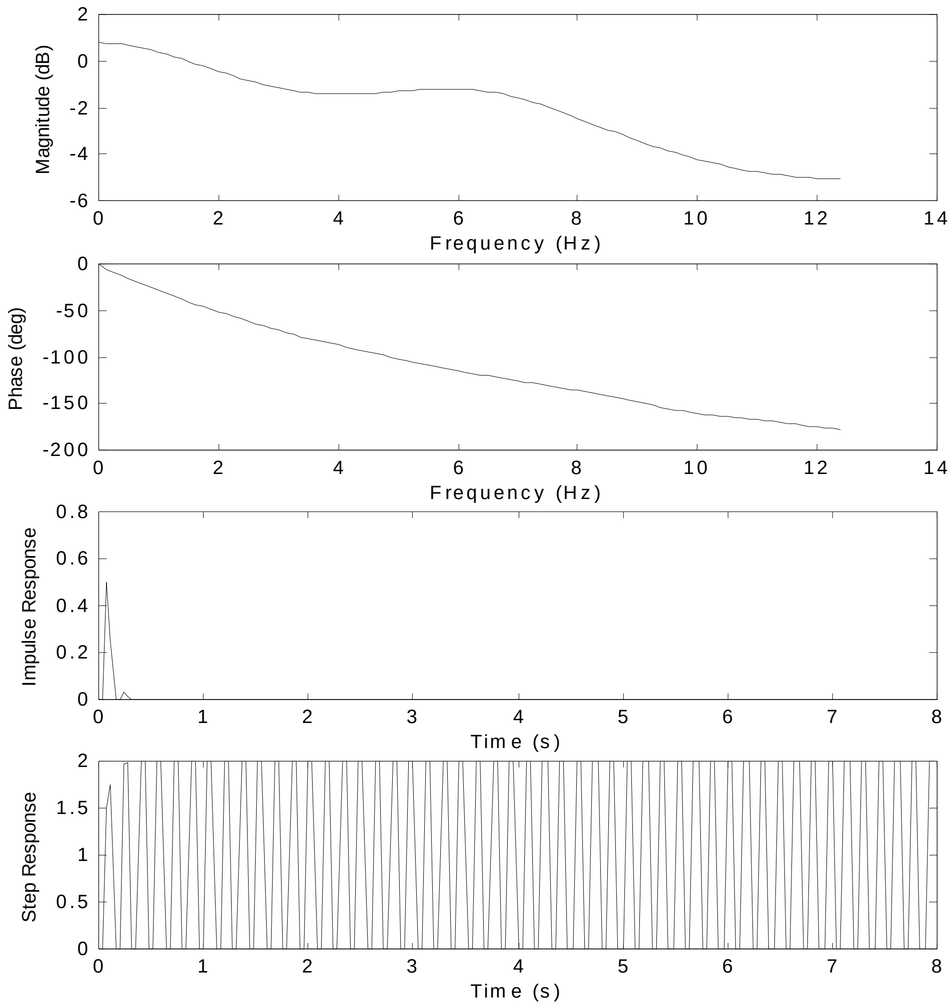

Figure 9. Bode diagrams, impulse and step responses for system with TV output matrix and A(k)=0.5.

The most important changes on amplitude diagrams in respect to matrices **B** and **C** are:

a) New maximum corresponding to frequency of **C**(k) equal to 1/(0.04·4)=6.25 Hz

b) Magnitude for f=0 approximately equal to 1 dB - about 2 dB higher damping than for example 4.2. Such damping is caused by stronger relationship with mean of **C**(k) than with power of **B**(k).

The relationship of steady state magnitude with mean of **C**(k) is not coincidence.

Similar simulation has been carried out for matrix A(k)=0.9. The results are depicted on fig. 10. Amplitude plot clearly shows new maximum for f=6.25 Hz.

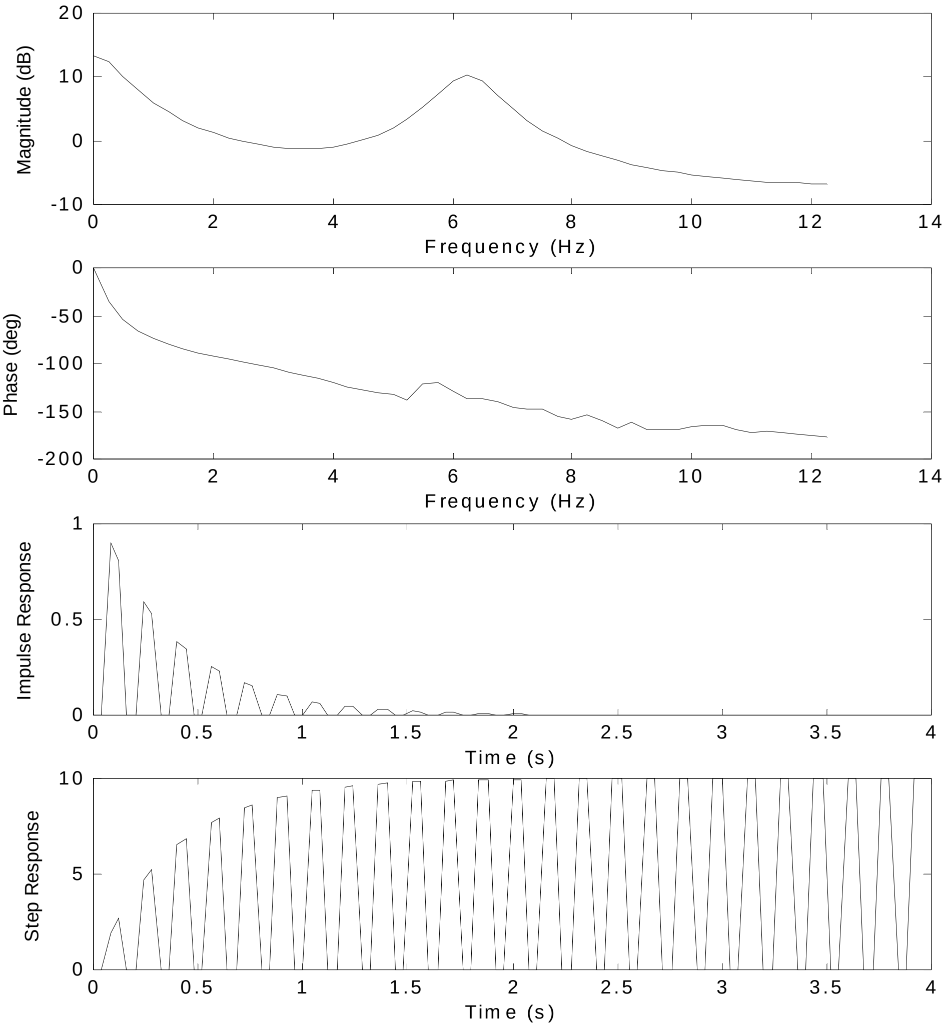

Figure 10. Bode diagrams impulse and step responses for system with TV output matrix and A(k)=0.9.

4.6 Negative system with TV input-output matrices

Joining examples 4.2 and 4.5, system matrices take following form

$$\mathrm{A}(k) = 0.5,\ \mathrm{B}(k) = -\Pi\left(\frac{k}{4}\right),\ \mathrm{C}(k) = \Pi\left(\frac{k}{4}\right) \tag{12}$$

Corresponding diagrams are depicted on fig. 11. Such variability of system matrices follows to drastic changes on amplitude and phase diagrams. Moreover it can be seen phase shift 180 deg owing to negative amplification.

Diagrams for matrix A(k) equal to -0.5 are depicted on fig. 12.

Of course for singular case A(k)=0, both Bode diagrams, impulse and step responses are equal to zero.

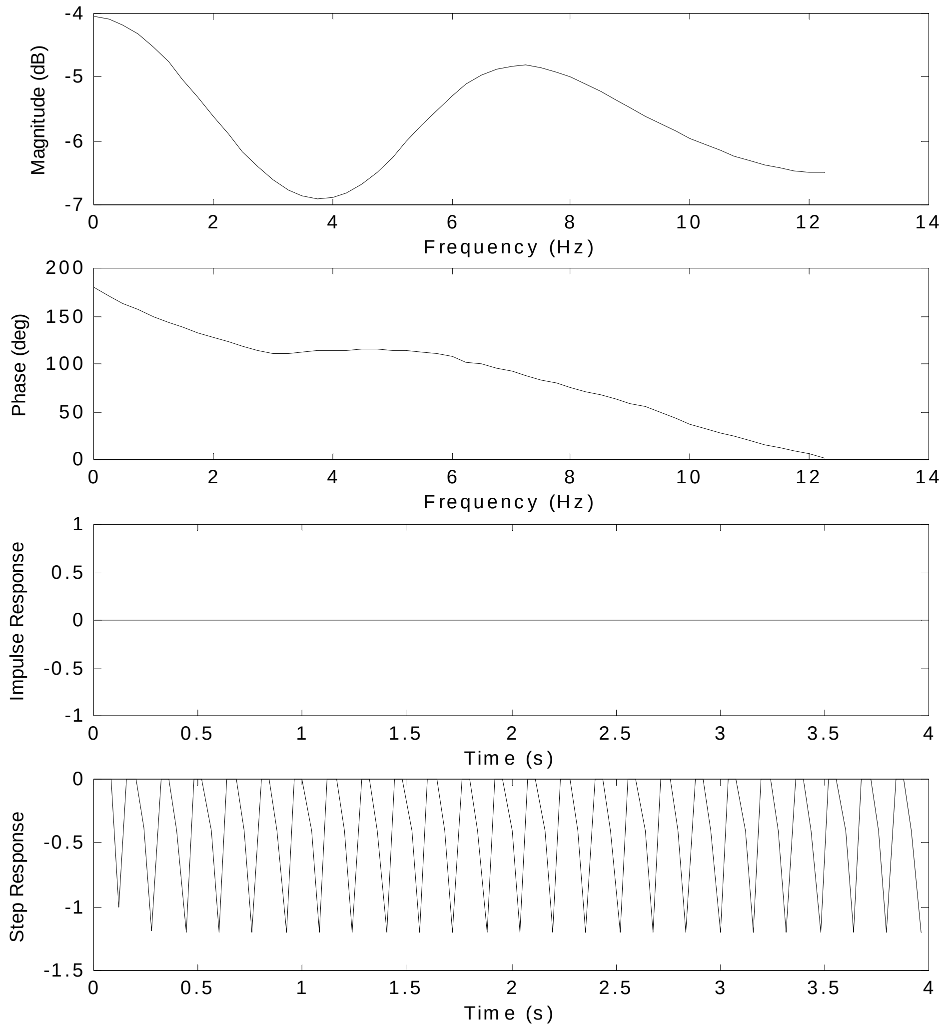

Figure 11. Bode diagrams, impulse and step responses for negative TV input-output matrices and A(k)=0.5.

4.7 System with TV state matrix

The last example shows third possible case – time varying matrix A(k). It is the more difficult to analyse among the three examples considered in the paper. Matrices of the model take following form

$$\mathrm{A}(k) = \Pi\left(\frac{k}{4}\right) + 0.5,\ \mathrm{B}(k) = 1,\ \mathrm{C}(k) = 1 \tag{13}$$

Corresponding diagrams are depicted on fig. 13 and following properties of them can be noted: Level of amplitude plot is raised by unstable part of signal A(k). Starting level for f=0 read off from fig. 13 is approximately equal to 18.7 dB. Average amplification read off from step response is approximately equal to 9. Due to such observations the values can be recognized as adequate. Maximum on amplitude plot corresponds to frequency of **A**(k) 1/(0.04·4)=6.25 Hz. Interesting may be comparison between fig. 13 and fig. 10. Amplitude diagrams are similar but the differences can be easily seen on phase plot. The phase diagram for system with TV output is monotonic but for system with TV system matrix has 2 clear phase jumps. Also impulse and step responses differ clearly. For the case from fig. 13 the responses are close to the system with TV input matrix.

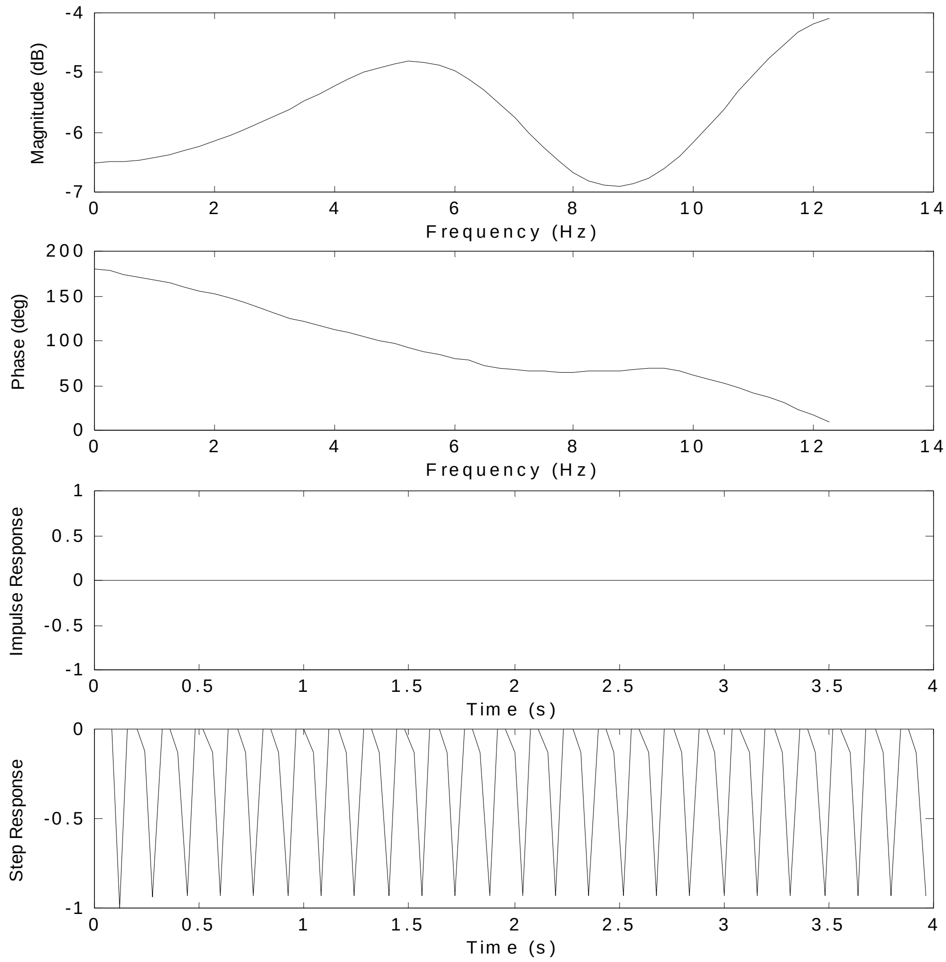

Figure 12. Bode diagrams, impulse and step responses for negative TV input-output matrices and A(*k*)=-0.5.

5 CONCLUSION

Dynamical properties of LTV systems can be easily explored using the SVD-DFT based method in similar way as using classical Bode diagrams for LTI systems. Four simultaneously obtained diagrams for LTV systems allow to carry out complex analysis of LTV systems in a much less complicated way than using other known methods, e.g. time-varying transfer function [Kozek, 1997] or psudomodal parameters [Maia, 1997], [Liu, 1999]. Limited amount of information that can be contained into the diagrams causes that some information is neglected. For example for time-varying input matrix, the variability of the systems does not transfer directly to the frequency diagrams but one can observe only the power of the signal controlling changes in the input matrix. In the case of variability in the output or system matrices one can observe the maximum magnitude for a frequency corresponding to the input signal and its harmonics.

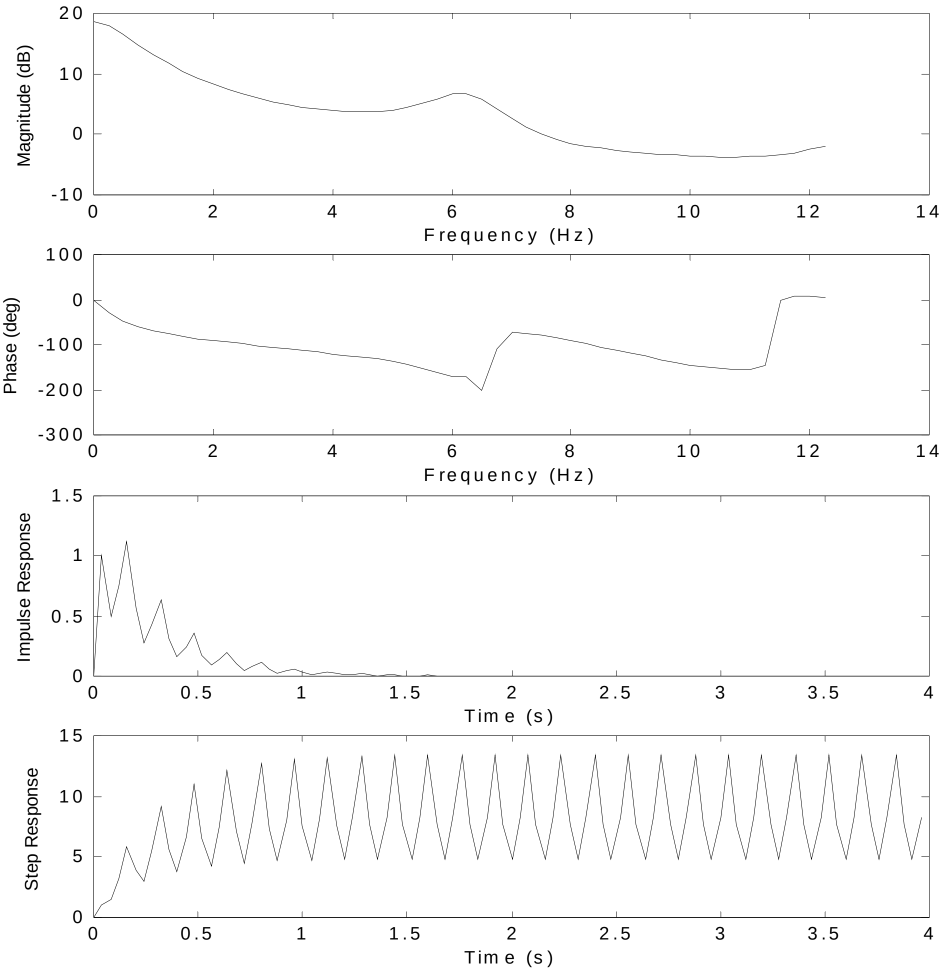

Figure 13. Bode diagrams determined for system with TV state matrix.

References

KOZEK, W. 1997. On the generalized transfer function calculus for underspread LTV channels. *IEEE Trans. Signal Proc.*, 1997, **45**, 219-223.

LIU, K. 1999. Extension of modal analysis to linear time-varying systems. *Journal of Sound and Vibration,* 1999, **226**, 149-167.

MAIA, N. M. M.; SILVA, J. M. M. 1997. *Theoretical and Experimental Modal Analysis*. New York. 1997. John Wiley&Sons Inc.

ORŁOWSKI, P. 2001. Applications of Discrete Evolution Operators in Time-Varying Systems, *Proc. of the European Control Conference*, Porto, Portugal, 2001, pp. 3259-3264.

ORŁOWSKI, P. 2003. An introduction to SVD-DFT frequency analysis for time-varying systems. *Proc. of 9th IEEE Int. Conf. MMAR 2003*. Międzyzdroje, Poland, 2003, pp. 455-460.

ORŁOWSKI, P. 2004. Selected problems of frequency analysis for time-varying discrete-time systems using singular value decomposition and discrete Fourier transform. *Journal of Sound and Vibration*, 2004, **278**, 903-921.